

Kimberlites: Magmas or mixtures?

Michael Patterson^{a,*}, Don Francis^a, Tom McCandless^b

^a Department of Earth and Planetary Science, McGill University, 3450 University Street, Montreal, Quebec, Canada H3A 2A7

^b Stornoway Diamond Corporation, Suite #800-625 Howe St., Vancouver, British Columbia, Canada V6C 2T6

ARTICLE INFO

Article history:

Received 29 September 2008

Accepted 1 June 2009

Available online 21 June 2009

Keywords:

Kimberlite magma
Harzburgite mantle
Olivine chemistry
Kimberlite petrogenesis
Mantle fluids
Diamond exploration

ABSTRACT

Although the presence of xenocrystic olivine is widely recognized in kimberlite, there is little consensus about its contribution to the existing estimates for the composition of kimberlite magma. Whole rock geochemistry is critical to the debate regarding the composition of kimberlite magma, however, it has received little attention as an indicator of diamond grade due to conventional thought that diamonds are xenocrysts unrelated to their host kimberlite. The Foxtrot kimberlite Field in Northern Québec is comprised of at least three distinct kimberlite intrusions exhibiting variation in both diamond grade and geochemistry making it an ideal suite with which to test a possible correlation between diamond grade and whole rock composition. Olivine is ubiquitous (30 to 70%) in the Foxtrot kimberlites and exhibits a restricted composition that overlaps that of olivine in harzburgite xenoliths suggesting that the majority of olivine is xenocrystic. Carbonate is also abundant (8 to 35%) in the Foxtrot kimberlites and exhibits magmatic textures requiring that carbon be considered in any petrogenetic model for the Foxtrot kimberlites. Pearce element ratio analysis assuming P as a conserved element indicates that much of the major element variation in the Foxtrot kimberlites can be explained by variable amounts of olivine and orthopyroxene in proportions (~80/20), similar to that of cratonic mantle xenoliths. The xenocrystic nature of olivine requires that the contribution of mantle harzburgite must be removed to constrain the composition of the magma. The calculated magma composition that results from the mathematical removal of olivine and orthopyroxene (80/20) from the whole rock compositions is significantly poorer in MgO (15 wt.%) and silica (~24 wt.%), but CO₂ rich (~17 wt.%) compared to previous estimates for kimberlite magma. The Foxtrot kimberlites are best modelled as mixtures of harzburgite mantle and a relatively carbonate-rich magma. According to this model the correlation between whole rock composition and diamond grade reflects the fact that the diamonds are also xenocrystic and sourced in the harzburgite component.

© 2009 Elsevier B.V. All rights reserved.

1. Introduction

The alkaline ultramafic rocks known to host diamonds share the unusual characteristic of being highly enriched in incompatible trace elements, but highly refractory in terms of major element composition. Conventional wisdom in the diamond exploration industry is that diamonds are xenocrysts, unrelated to their host “kimberlites”. Because of this philosophical bias, along with their xenolith rich and fragmental nature, the chemical composition of kimberlitic host rocks has received relatively little attention as an exploration tool or as an indication of diamond grade. The present classification of alkaline ultramafic rocks is a confusing mineralogical legacy that is complicated by geographic parochialism. However, a survey of the existing chemical analyses of hypabyssal-facies alkaline ultramafic rocks suggests they can be reliably distinguished on the basis of their silicon and iron contents and that these major element differences have important implications not only for their classification, but also for the nature of their mantle source

regions, and even their diamond potential (Francis, 2003; Francis and Patterson, 2009). There are now four independent studies suggesting that there is a relationship between the bulk composition of a kimberlite and its potential diamond grade, with the highest diamond grades associated with the lowest bulk rock iron and titanium contents (Vasilenko et al., 2002; Francis, 2003; Birkett et al., 2004; Hartzler, 2007). This finding is consistent with the rule of thumb of prospectors that kimberlites rich in titanomagnetite do not carry diamonds. This anti-correlation defies conventional wisdom that kimberlites simply transport diamonds to the surface, and are genetically unrelated to their precious cargo. In any case, it appears that a simple whole rock major element analysis is sufficient to uniquely classify “kimberlitic” rocks, and may provide an inexpensive tool for the preliminary evaluation of their diamond potential.

The Foxtrot Kimberlite Field is a diamond play in the Otish Mountains of Québec that is operated by a joint venture between Stornoway Diamond Corporation and SOQUEM. The Foxtrot Kimberlite Field consists of at least 9 different kimberlite pipes, known collectively as the Renard cluster, as well as two other distinct dykes known as the Lynx dyke system and the Hibou dyke (Birkett et al., 2004). The Renard bodies comprise brecciated diatreme cores cut by late stage dykes and sills of hypabyssal

* Corresponding author.

E-mail address: bodhi123@eps.mcgill.ca (M. Patterson).

kimberlite. There is a wide range of kimberlite compositions and diamond grade in the Foxtrot Kimberlite Field, offering a unique opportunity not only to test the proposed chemical classification of kimberlitic rocks, but also to investigate possible correlations between kimberlite composition and their diamond grade. Our results indicate that kimberlites are best regarded as mixtures whose whole rock composition and diamond grade reflect the type and amount of lithospheric mantle that the Foxtrot kimberlites have entrained.

2. Geologic setting

2.1. Regional geology

The Foxtrot bodies were emplaced into Archean metamorphic rocks of the eastern Superior Province (Fig. 1). The northern portion of the property is underlain by North–Northwest trending, plutonic and gneissic terranes (varying in width from 70 to 150 km) defined by metamorphic grade, lithology, and aeromagnetism (Clements and O'Connor, 2002). The basement gneiss near the Foxtrot bodies has been metamorphosed at upper amphibolite to lower granulite facies conditions in late Archean time (Birkett et al., 2004). Pleistocene glaciation of the Foxtrot area has left thick till deposits, lag deposits of glacially transported boulders, and large glacial erratics. Among the glacial erratics are a large number of kimberlite boulders, which were used as an exploration tool to locate kimberlite dykes on the property.

A perovskite U–Pb age of 631.6 ± 3.5 Ma has been obtained for a hypabyssal dyke cutting the Renard 1 pipe and composite age of $640.5 \pm$

2.8 Ma for three hypabyssal dykes cutting the Renard 2 and 3 pipes (Birkett et al., 2004; Fitzgerald et al., this issue). This is similar to the 629 ± 29 Ma age reported for the Wemindji kimberlites that are approximately 400 km to the West of the Foxtrot Kimberlite Field. A significantly younger age of 522 ± 30 Ma was obtained, however, on groundmass ilmenite in the Lynx dyke (McCandless et al., 2008). Other nearby kimberlite occurrences in the Otish Mountains include the Lac Beaver and Tichegami kimberlites that occur approximately 70 km to the South of the Foxtrot Kimberlite Field with an age of 551 ± 3 Ma (Girard, 2001; Moorhead et al., 2002; Letendre et al., 2003).

2.2. Detailed geology

The Foxtrot Kimberlite Field is comprised of at least three distinct kimberlite occurrences in terms of emplacement morphology, geochemistry, and mineralogy. The field is dominated by nine diatreme pipes that form the Renard cluster in the eastern portion of the field (Fig. 1). These pipes are individually elongated along the north north-west trend collectively defined by the pipes. The pipes are primarily composed of transitional to diatreme facies kimberlite that is intruded along facies boundaries and pipe margins by late stage hypabyssal kimberlite dykes (Birkett et al., 2004; Fitzgerald et al., this issue). The Lynx dyke system is located two km to the West of the Renard cluster, but shares the north north-west orientation of the Renard pipes, whereas the Hibou dyke system, located between the Renard cluster and the Lynx dyke system, has an approximate east–west orientation (Fig. 1). Other kimberlite occurrences related to the Foxtrot Kimberlite Field

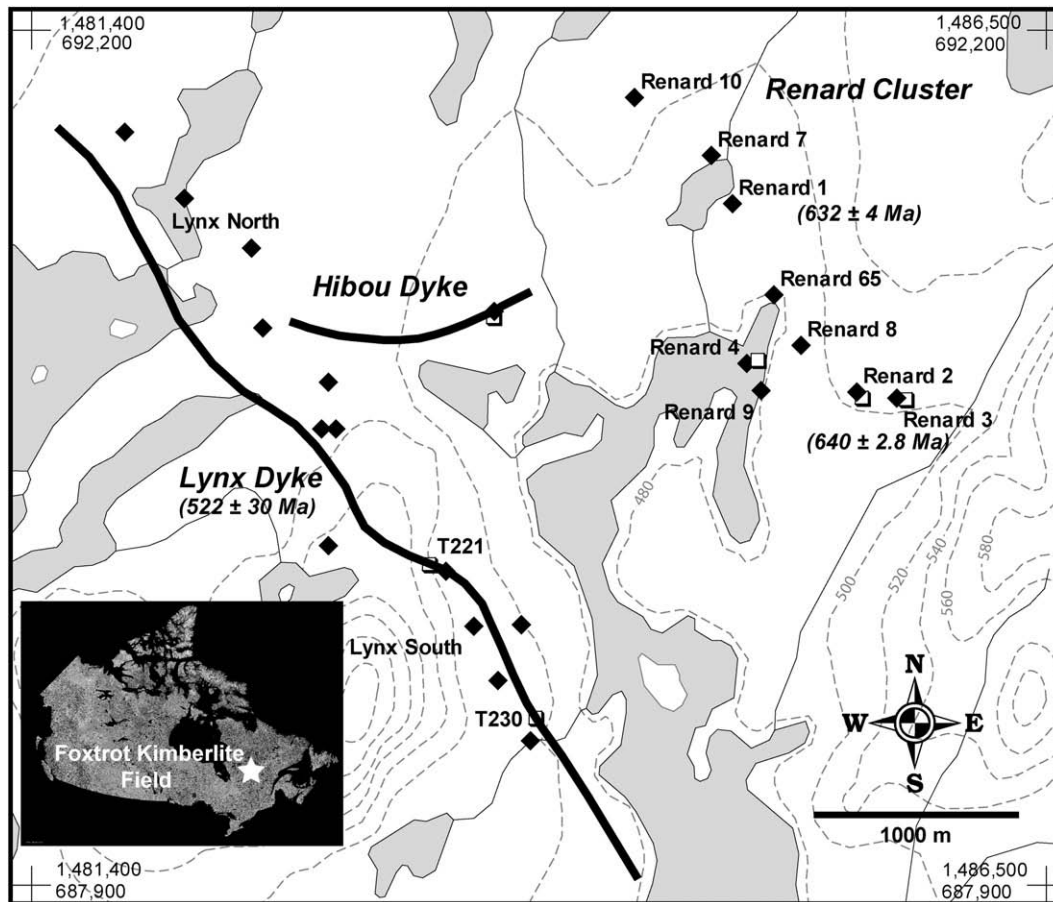


Fig. 1. Location map for the Foxtrot Kimberlite Field indicating Renard cluster of kimberlite pipes (black diamonds — center coordinates of pipe) in upper right of map; interpreted surface expression of the Lynx dyke indicated by black line and intersecting drill hole locations (black diamonds adjacent to line); interpreted surface expression of the Hibou dyke indicated by black line. Open trench or drift sample site indicated by open squares. Foxtrot Kimberlite Field location shown on image of Canada (inset).

include the North Anomaly dyke located ~5 km to the North of the Renard cluster and the Southeast Anomaly dyke located ~3 km South-east of the Renard cluster.

The Renard kimberlite pipes are steep-sided diatreme pipes with irregular contacts with the host country rock that have been encountered in drill core to a depth of 500 m. This morphology is consistent with the root zone in Class 1 (Kimberley type) kimberlite pipe models (Hawthorne, 1975; Clement, 1982). Class 1 kimberlite pipes typically consist of three zones; a crater zone close to the surface, a diatreme zone with the archetypical carrot shape, and a root zone at depths between 800 m and 1300 m below the crater (Hawthorne, 1975; Clement, 1982). Rare fragments of siltstone and carbonate presumed to be derived from the Proterozoic cover rocks of the Otish Group have been found in volcanoclastic breccia units of Renard 65 (Clements and O'Connor, 2002). The Otish Group has a stratigraphic thickness of approximately one km, and the presence of these rare sedimentary xenoliths indicates that, at the time of the kimberlite emplacement, the gneissic basement was covered by the Otish Supergroup. The lack of Otish Supergroup outcrops indicates that the current surface exposure of the Renard kimberlite pipes represents a level at least one km below the surface at the time of emplacement, near the typical transition between the root zone and diatreme zone.

The diatreme pipes are composed dominantly of volcanoclastic kimberlite, with a high proportion of xenoliths of the granitoid country rock (Birkett et al., 2004; Gofton, 2007; Fitzgerald et al., this issue). Marginal zones of brecciated country rock (\pm kimberlite) of variable width surround the diatreme pipes (Fitzgerald et al., this issue). In addition to the diatreme infill, there is also a subordinate amount of coherent kimberlite that is texturally complex and has fewer xenoliths of granitoid country rock (Fitzgerald et al., this issue). The coherent kimberlite occurs predominantly in the form of hypabyssal kimberlite (HK) dykes (<1 m), but also as irregular intrusions, that are found throughout the body. The HK dykes are zoned with medium to very dark grey kimberlite interiors that grade to rusty-orange margins that are rich in phlogopite and clinopyroxene. The presence of narrow hypabyssal kimberlite dykes and sills throughout the Renard pipes is consistent with the present erosion level corresponding to the transition between the root and diatreme zones (Birkett et al., 2004; Gofton, 2007; Fitzgerald et al., this issue).

The Lynx dyke system comprises a series of semi-continuous, en echelon dykes, with an average thickness of ~1.8 m and a maximum thickness of ~3 m that can be traced nearly four kilometers along strike length. The system incorporates three different zones designated Lynx North, Lynx, and Lynx South (Fig. 1; Stornoway internal report) and is encountered along strike to the North and South, as well as at depth. Open trench excavation in the Lynx South zone reveals that the dyke is zoned with fine-grained margins and coarse grained (<10 mm) olivine-rich interiors. The Lynx dyke does not have any volcanoclastic kimberlite and there is no evidence of the dyke having breached the surface.

The Hibou dyke is interpreted to have an average thickness of ~2 m, a WNW strike length of at least 850 m and an approximate dip of 10° to the NNE. Drill core intersections indicate that the dyke exhibits similar fine-grained margins to those of the Lynx dyke, with sharp to gradational contacts with the coarser grained interiors. A lack of volcanoclastic kimberlite indicates that the Hibou dyke like the Lynx dyke, did not breach the surface.

3. Methods

Eighty-nine samples of hypabyssal dykes were collected from drill core and surface exposures of the Renard kimberlite pipes, the Lynx dyke, as well as boulders of the Hibou dyke. Complete transects across dykes were sampled in three locations, two across the Lynx dyke (13 samples) and a third across a dyke cutting the Renard 4 pipe (6 samples). Blocks (~100–400 cm³) were cut to minimize the effect of alteration and/or

contamination. These blocks were then crushed to approximately 10 mm and fresh inclusion-free fragments were picked using a binocular microscope to avoid xenolith contamination. The samples were dried at 60 °C, pulverized to 150 μ m using an alumina ring-and-puck grinder and analyzed for whole rock geochemistry by X-ray fluorescence using fused bead (major elements) and pressed-pellet techniques (select trace elements) developed at McGill University. A subset was analyzed for additional trace elements (including REE) by ICP-MS at Activation Laboratories Ltd. in Ancaster, Ontario.

Major element analyses of minerals in thin section were performed using a JEOL8900 electron microprobe at McGill University. Silicate grains were analyzed using an accelerating voltage of 20 kV, a beam diameter of 5 μ m, a beam current of 20 nA, and a maximum counting time for each element of 40 s. Oxide grains were analyzed using an accelerating voltage of 20 kV, a beam diameter of 5 μ m, a beam current of 20 nA, and a maximum counting time for each major cation of 20 s. Carbonate minerals were analyzed using an accelerating voltage of 15 kV, a beam diameter of 10 μ m, a beam current of 20 nA, and a maximum counting time for each major cation of 20 s. All analyses were corrected using standard ZAF corrections.

The whole rock and mineral chemical data have been converted to cation units by applying the equation;

$$\text{cat} = \frac{\text{Oxide Wt\%}}{\text{Molecular Wt.}} \times \text{No. of Cations}$$

to all the oxides (i.e. SiO₂) and then normalizing the results to 100 cations. This allows whole rock data to be directly interpreted in terms of mineral (i.e. olivine, (Mg,Fe)₂SiO₄) stoichiometry in chemical variation diagrams. Carbon was included as a cation in the calculations because of the high modal abundance of carbonate with primary magmatic textures.

The exclusion of water in the cation calculation is based on the difficulty in distinguishing the contribution of magmatic water and meteoric water to the total water content of the kimberlite. Although water is undoubtedly important to kimberlite petrogenesis, studies of groundmass serpentine in kimberlites suggests that much of the whole rock water is meteoric (Sheppard and Dawson, 1975; Stripp et al., 2006). In any case, ignoring water in petrogenic studies is only a concern if there are hydrous phases, such as serpentine, at the magmatic stage (Francis and Patterson, 2009).

4. Results

4.1. Petrology

The dominant minerals of the Foxtrot kimberlites include olivine (variably serpentinized), calcite, dolomite, phlogopite, monticellite and ilmenite, while accessory minerals (~5% modal) include perovskite, spinel, and apatite, which have previously been described by Birkett et al. (2004). Olivine and carbonate alone account for 65 to 95% of the modal mineralogy of these rocks and control the compositional variation. The Renard dykes have carbonate contents (~8–35% modal) that are on average lower than those of the Lynx and the Hibou dykes (~15–35% modal). The Lynx dyke differs from the Renard and Hibou dykes in having higher modal ilmenite, a lower abundance of groundmass phlogopite, and in the lack fresh olivine. Fresh olivine is abundant in samples of the Hibou dyke, whereas the olivine of the Renard dykes range from completely altered to fresh olivine.

The Renard dykes are predominantly macrocrystic kimberlite, comprised of olivine crystals that range from ~10 mm to micron-scale set in a fine-grained matrix of phlogopite, monticellite, spinel, perovskite and apatite. A subset of Renard dyke samples have a low abundance of macrocrystic olivine and abundant phlogopite and clinopyroxene, giving the rocks a rusty-orange color. These rusty-orange samples are typically located within 30 cm of contacts juxtaposed with volcanoclastic kimberlite. The Lynx dyke is also macrocrystic kimberlite with the

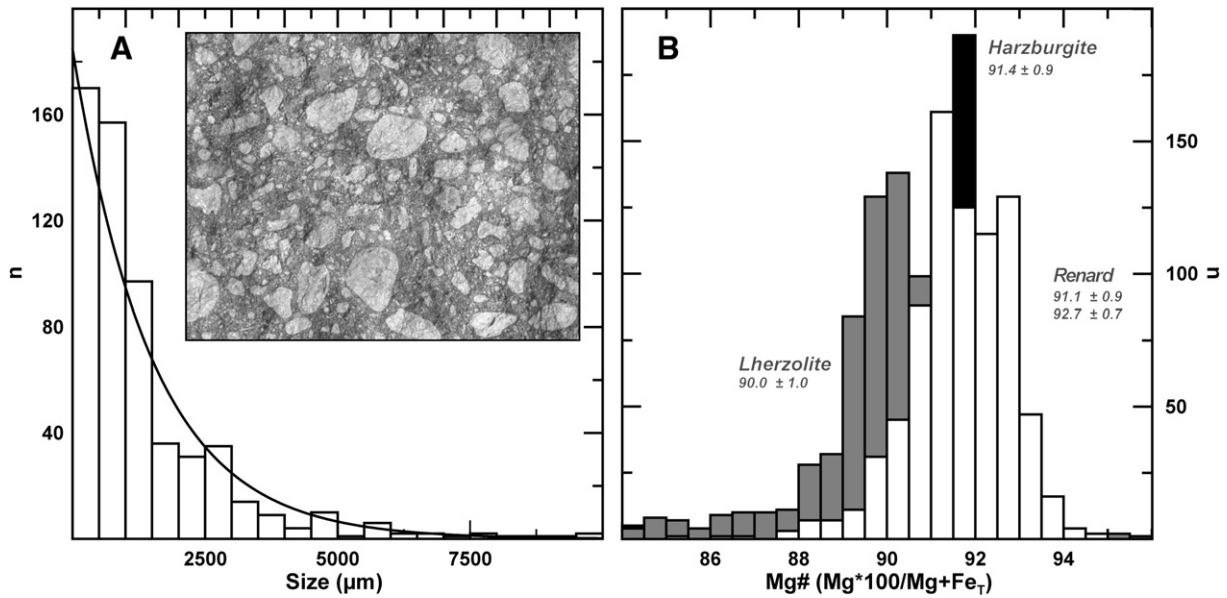


Fig. 2. (A) Histogram of olivine sizes in thin section (longest axis) with exponential best fit line. Inset: Photograph of Lynx dyke interior sample, olivine as ovoid to irregular shapes with light gray color set in darker gray carbonate matrix, fov ~25 mm. (B) Mg# histogram of olivine from the Renard dykes (white bars) compared with harzburgite (black bars) and lherzolite (grey bars) (modes as indicated on diagram). Peridotite data from GEOROC online database filtered for olivine from lherzolite and harzburgite mantle xenoliths.

larger olivine of the dyke interior commonly exhibiting a preferred orientation with their long axes sub-parallel to the dyke margins (Supplementary Fig. 1). Strongly magnetic carbonate veins typically exhibit red staining are common within the macrocrystic interiors of the Lynx dyke, suggesting that post-emplacment fluids remobilized iron in the system. The Lynx dyke has thin aphanitic margins (<20 cm) that exhibit both sharp and gradational boundaries with the coarser grained interiors of the dyke. Serpentine in the aphanitic margins is fine grained (<1 mm) and is set in a matrix of carbonate and micron-scale euhedral to subhedral magnetite and chromite. Centimetre-scale cyclic banding defined by the concentration of opaque oxides parallels the dyke contact often accompanied by parallel carbonate veinlets. Large serpentinized olivine grains (~2 mm) within the fine grain margins that exhibit a high aspect ratio are preferentially aligned parallel to the dyke margins.

Olivine and its pseudomorphs are ubiquitous in all the hypabyssal dykes, forming from 30 to 70% of their mode. The colour of the olivine grains ranges from dark green to pale greenish white, reflecting the varying degree of serpentinization and calcification. Complete pseudomorphing by serpentine is typical for the smaller crystals, but partial to complete serpentinization affects all grain sizes. Both fresh olivine crystals, and well preserved serpentinized pseudomorphs, display ovoid to subhedral habits. An analysis of more than 800 olivine crystals indicates that there is an exponential decrease in abundance from crystals less than 100 μm in size to 10 mm (Fig. 2A). Transects across the Lynx dyke indicate that the maximum olivine grain size (<10 mm) occurs in the center of dyke and that grain size decreases toward the dyke margins (<2 mm). Although fresh olivine is common in the Renard dykes, and abundant in the Hibou dyke, it is

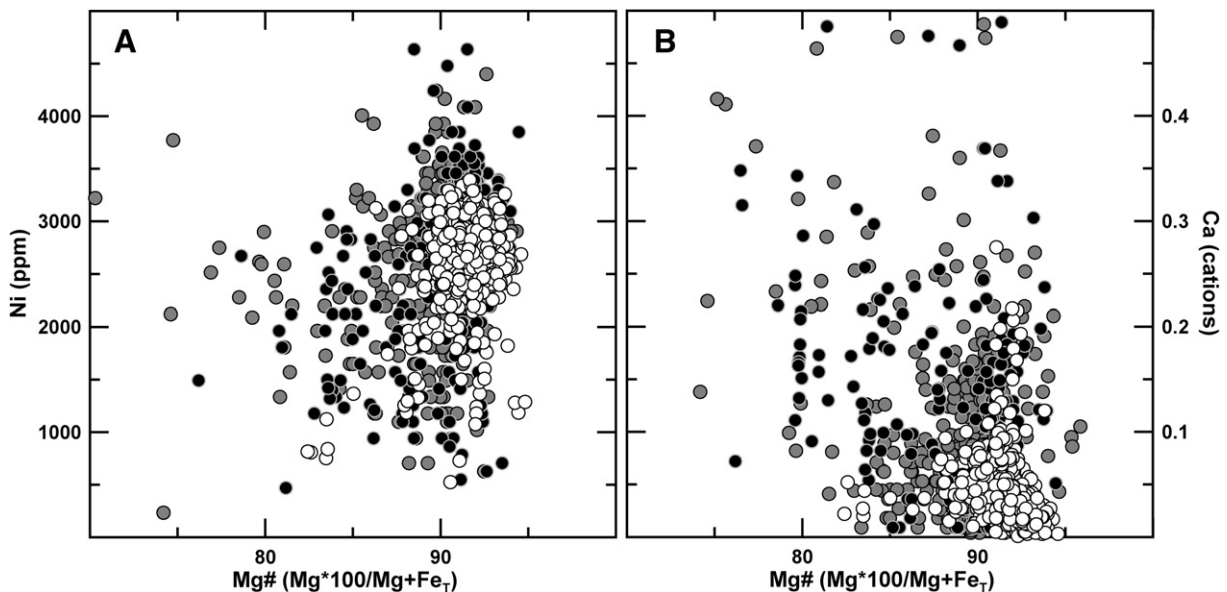


Fig. 3. (A) Plot of Ni versus Mg# for Foxtrot olivine chemistry compared with harzburgite and lherzolite olivine chemistry. (B) Plot of Ca versus Mg#, same data set as in A. Background data (harzburgite and lherzolite) from GEOROC online database filtered for olivine with mantle origin. Gray circle – lherzolite olivine; black circle – harzburgite olivine; white circle – Foxtrot kimberlite olivine.

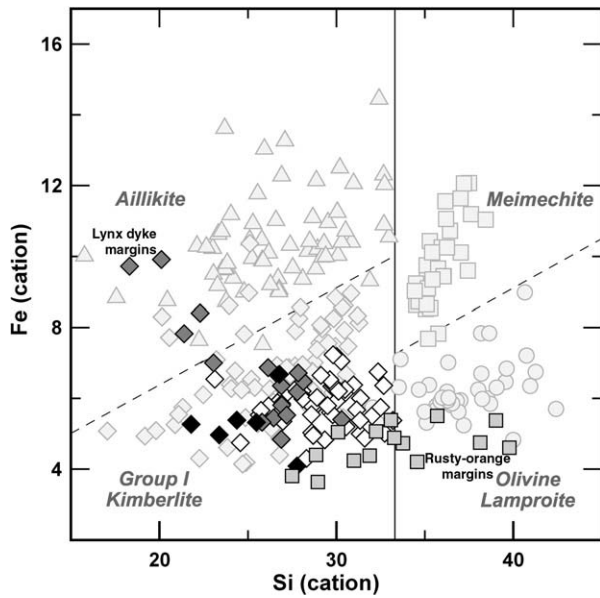


Fig. 4. Plot of Fe versus Si with ultramafic lamprophyres fields after Francis and Patterson (2009). White diamond – Renard dykes; light gray square – Renard dyke margins; dark gray diamond – Lynx dyke; black diamond – Hibou dyke; background symbols as indicated (data from Francis and Patterson, 2009).

absent in the rusty-orange margins of the Renard dykes and the Lynx dyke.

The compositional range of the olivine is relatively restricted, but is distinctly bimodal in terms of Mg# ($Mg \times 100 / (Mg + \Sigma Fe)$) with modes at 91.1 ± 0.9 and 92.7 ± 0.7 (Fig. 2B). The majority of the olivine grains (95%) have nickel contents ranging from 2200 to 3400 ppm, exhibiting a single mode at ~2900 ppm, with the remaining 5% of the olivine ranging down to 500 ppm (Fig. 3A; Supplementary Table 3). The calcium contents of the Foxtrot olivine is uniformly low, ranging from less than detection limit (0.03) to 0.28 cations (Fig. 3B). None of these chemical parameters show any correlation with grain size.

Carbonate is the second most abundant phase in the Foxtrot hypabyssal dykes, accounting for between 8 and 35% of the rock and

dominating the interstitial groundmass (40–80%). Although both dolomite and calcite are present in all samples, calcite is typically dominant. The most distinctive magmatic textures are observed in the Lynx dyke, where calcite occurs as millimeter scale oikocrysts that enclose small olivine and other matrix minerals (Supplementary Fig. 1G). A subset of the Foxtrot kimberlites contain micron-scale euhedral dolomite rhombs that commonly form larger clusters within the matrix (Supplementary Fig. 1H). Both calcite oikocrysts and dolomite rhombs also occur in fresh samples of the Hibou dyke and the Renard dykes.

Phlogopite is a minor phase (<5%) in all Foxtrot dykes occurring as dispersed macrocrysts up to 5 mm in size and small groundmass crystals characterized by subhedral to euhedral plates that range in size from 5 to 10 μm . Groundmass phlogopite is more abundant in the rusty-orange margins of the Renard dykes, where it typically forms haloes around fragments of quartz, feldspar, and muscovite that are interpreted to be crustal xenoliths (Supplementary Fig. 1C and 1D). The groundmass phlogopite grains are randomly orientated and commonly display euhedral to irregular cores with euhedral overgrowths, although a clear distinction between core and overgrowth is not always possible.

The phlogopite in the Renard dykes exhibits a large compositional variation within and between individual dykes (Supplementary Table 2). The majority of the core compositions, however, correspond to the field of kimberlite phlogopite as defined by Mitchell (1995, 1997) in terms of aluminium (~14–19 wt.%) and iron (~3–6 wt.%) contents (Supplementary Fig. 2). Phlogopite in the interior of the Renard dykes have Mg#s that range from ~95 to 82 (assuming all Fe as Fe^{2+}) with a concomitant decrease in aluminium with decreasing iron. The mica within the rusty-orange margins of the Renard dykes, however, have a much smaller range of Mg#s (~92–52) and have compositions that range from the kimberlitic field towards the composition of tetraferriphlogopite.

Clinopyroxene is only found in the rusty-orange margins of the Renard dykes and typically occurs as small (<30 μm) euhedral microlites, but also as rare crystals up to 100 μm , commonly associated with groundmass phlogopite. Despite its small grain size, clinopyroxene can be modally significant in the rusty-orange margins, reaching 35% in one sample. The smaller clinopyroxene crystals (<30 μm) commonly display euhedral to subhedral prismatic habits and frequently exhibit compositional zoning. Larger clinopyroxene crystals exhibit cyclically-zoned mantles developed

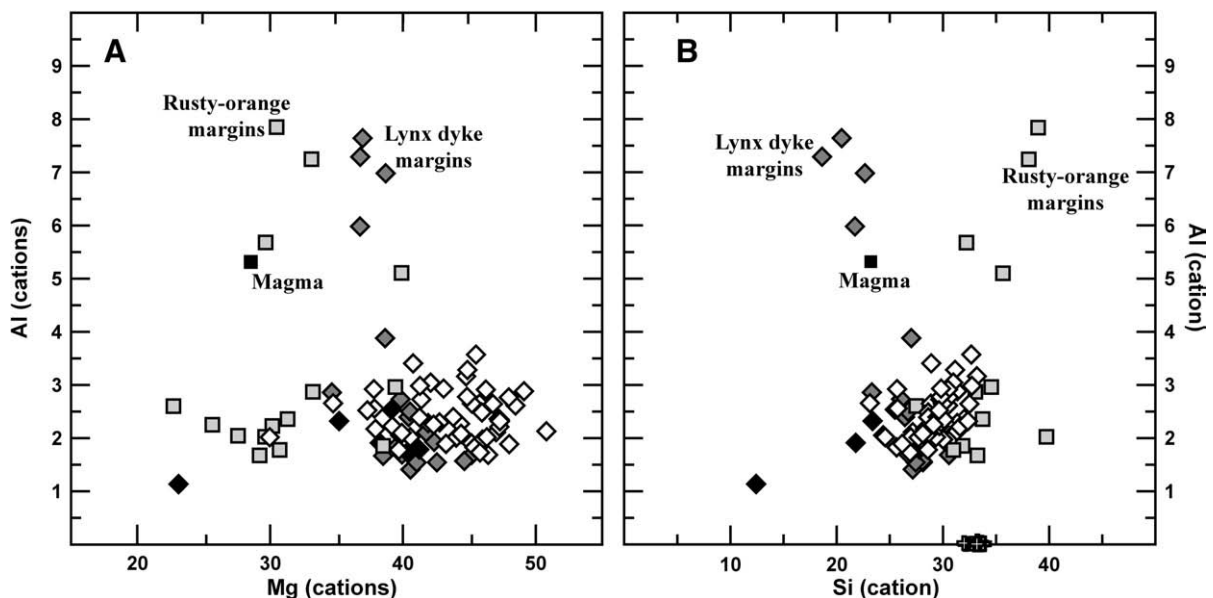


Fig. 5. Foxtrot whole rock geochemical plots; (A) Al versus Mg illustrating concomitant decrease of Al with decreasing Mg for fresh macrocrystic kimberlite and increasing Al with decreasing Mg for both Lynx dyke and Renard dyke margin samples; (B) Al versus Si illustrating concomitant decrease of Al with decreasing Si for fresh macrocrystic kimberlite and increasing Al with increasing Si for the rusty-orange margins of the Renard dykes, whereas Al increases with decreasing Si in the Lynx dyke margins. Symbols same as in Fig. 4.

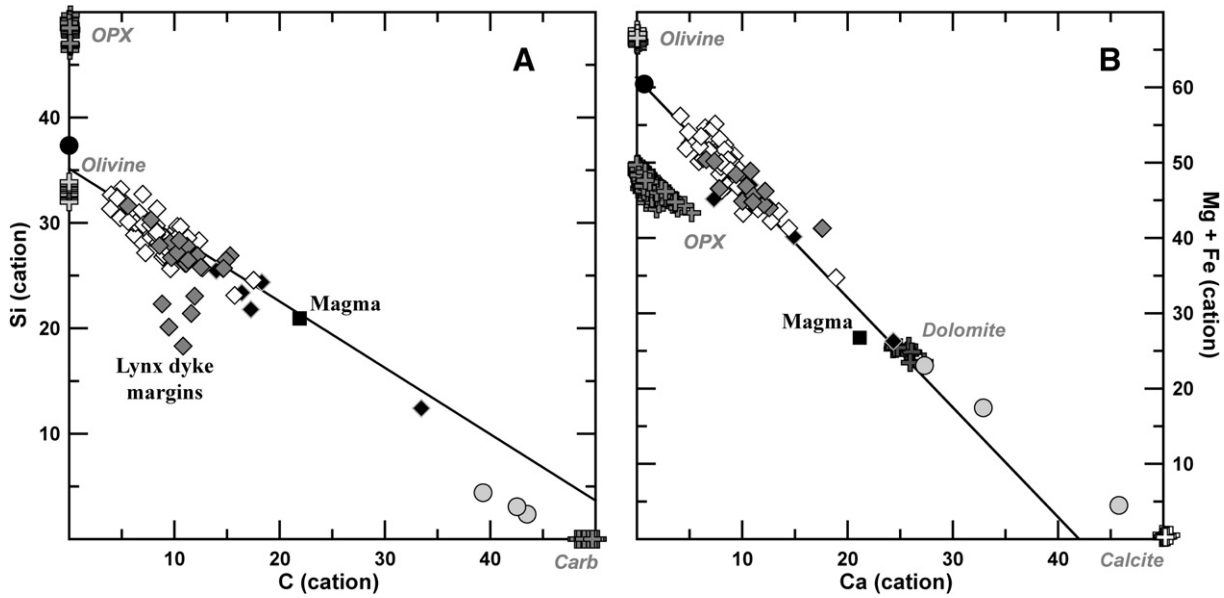


Fig. 6. Kimberlite whole rock data: (A) plot of Si versus C and (B) plot of Mg versus Ca; Foxtrot kimberlite symbols same as in Fig. 4; gray circles – average carbonatite (Woolley and Kempe, 1989); black circle – average mantle xenolith found in kimberlite, black square – estimated magma, minerals as indicated. (xenolith data sources: see text).

on euhedral to irregular cores (Supplementary Fig. 1F). The majority of the clinopyroxene plot within the diopside field of the pyroxene quadrilateral, but cores are typically more Fe-rich (Mg# ~84; assuming all Fe as Fe²⁺) than the mantles (Mg# ~92; Supplementary Table 2).

Spinel in the Foxtrot dykes occurs as both form discrete crystals with mantle overgrowths and as atoll-textured crystals. The cores of discrete spinel crystals and of the atoll-textured spinel grains exhibit a large compositional range, but, plot as aluminous magnesian chromite in the reduced spinel prism (Supplementary Fig. 3). The mantle overgrowths exhibit an even larger range in composition, from magnesio-ulvöspinel to pleonaste spinel. Some of the overgrowth compositions fall along the magmatic Trend 1 (magnesian ulvöspinel) of Mitchell's (1995) reduced spinel prism, however, others plot between Trend 1 and Trend 2 (titanomagnetite), similar to the magmatic spinel trend of the Kirkland Lake kimberlites (Supplementary Fig. 3).

4.2. Whole rock geochemistry

The majority of the analyzed kimberlite samples (49 Renard dyke, 19 Lynx dyke and 7 Hibou dyke) have contamination indices (C.I. = SiO₂ + Al₂O₃/MgO + K₂O; Clement, 1982) close to unity (~0.9–1.3), have low Ti (0.5–2 cat), Fe (4–8 cat), and Si (21–33 cat) contents, and fall in the field of Group I kimberlite in a plot of Fe versus Si (Fig. 4). In contrast, the rusty-orange margins of the dykes cutting the Renard pipes have C.I.'s greater than 1.5, with higher Si contents (27 to 40 cat), lower Fe contents (3.5 to 5.5 cat), that span the boundary between the Group I and Group II kimberlite fields in a plot of Si versus Fe (Fig. 4; Supplementary Table 1). Although the Lynx dyke samples all have C.I.'s ranging from 0.97 to 1.13, the interior samples have Fe and Si contents that are similar to those of the Renard and Hibou dykes, whereas the aphanitic margins have distinctly lower Si and higher Fe contents (Fig. 4). The aphanitic margins of the Lynx

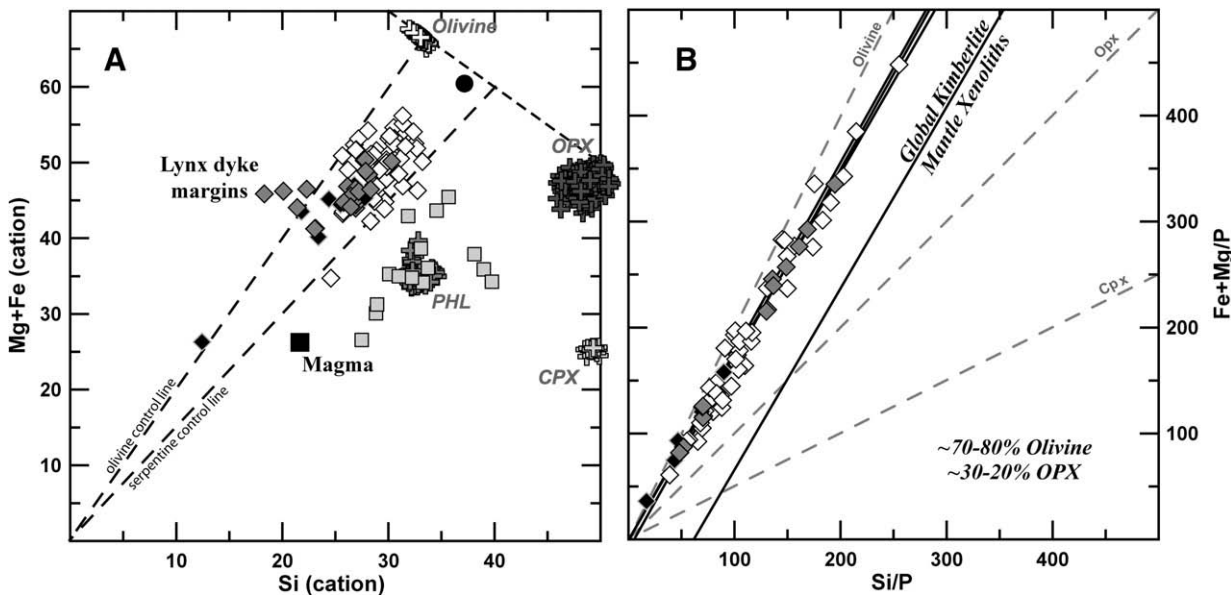


Fig. 7. (A) Plot of Mg + Fe versus Si for Group I kimberlite from the Renard dykes, Lynx dyke and Hibou dyke; olivine and serpentine control lines labeled dashed lines and dashed line in upper right is where cation Σ = 100. (B) (Fe + Mg)/P versus Si/P for Foxtrot kimberlites. Symbols same as Fig. 4, dashed lines indicate stoichiometric ratio for minerals as labeled.

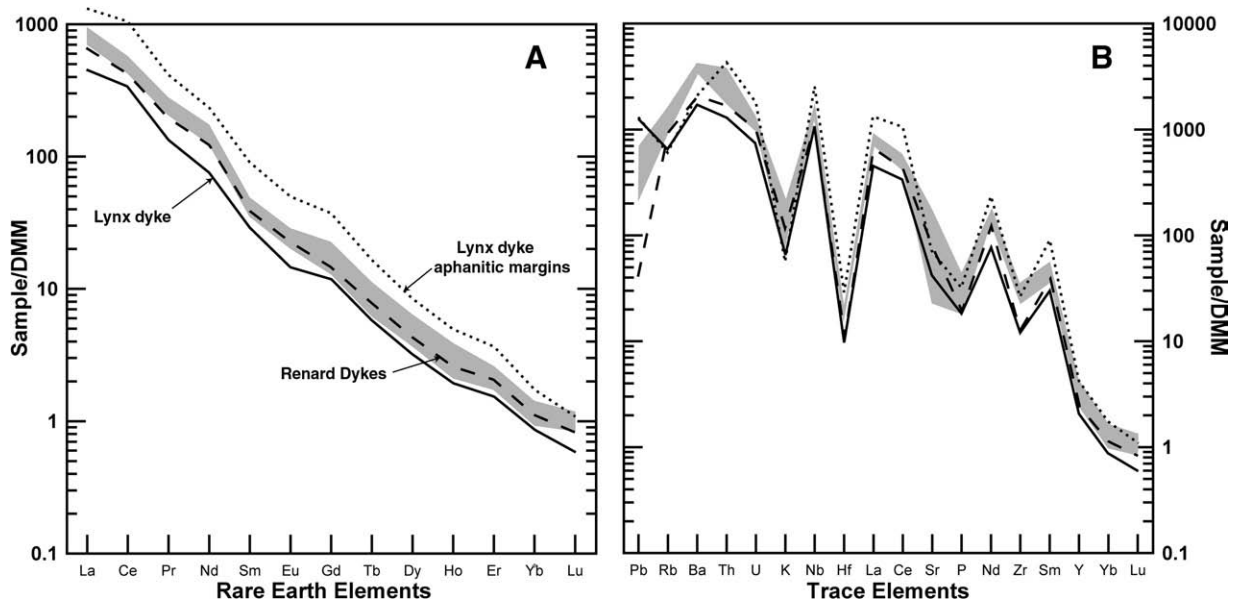


Fig. 8. Trace element spider diagrams comparing Renard dykes and Lynx dyke with trace element profiles Slave province kimberlites normalized to DMM (Workman and Hart, 2005). (A) REE profiles for the Renard dykes and Lynx dyke. (B) LILE and HFSE spider diagram for same samples. Gray shaded area – slave province Group I kimberlites (Price et al., 2000; Fedortchouk & Canil, 2004; Schmidberger & Francis, 2001); dashed line – Renard dykes average; solid line – Lynx dyke; dotted line – Lynx aphanitic margins.

dyke also have two to three times P, K, Ti, and Al contents than the crystal-rich interiors (Fig. 4 and 5). In contrast, the aphanitic margins have lower Mg and Si contents (37 ± 1 and 20 ± 2 cat respectively) than those of the dyke interiors (41 ± 3 and 28 ± 2 cat respectively).

The interiors of the Foxtrot hypabyssal kimberlites define an inverse linear trend in a plot of Si versus C that likely reflects mixing between carbonate and silicate phases (Fig. 6A). A plot of Mg + Fe versus Ca indicates that the silica-rich end-member of this trend corresponds to a mixture of olivine and orthopyroxene in the proportions $\sim 80/20$ (Fig. 6B), despite the fact that orthopyroxene is not an observed phase. Fresh Foxtrot kimberlite falls between the olivine and serpentine control lines in a plot of Mg + Fe versus Si and appear to define a common trend with refractory mantle xenoliths (Fig. 7A). The Foxtrot kimberlites also define a linear

trend in a Pearce element ratio (PER; Pearce, 1968; Russell and Nicholls, 1988) diagram, assuming phosphorus as the conserved element, that is consistent with variable amounts of olivine and orthopyroxene in proportions of $\sim 75/25$ (Fig. 7B). If clinopyroxene is included in the calculation, the ratio becomes $\sim 73/24/3$ (olivine/opx/cpx). This is consistent with the silica-rich end-member in Figs. 6 and 7 being the refractory mantle xenoliths commonly carried by kimberlite which have an average olivine to orthopyroxene ratio of $\sim 79/21$ ($n = 151$) (Nixon and Boyd, 1973; Carswell et al., 1979; Boyd, 1987; Boyd et al., 1997; Lee and Rudnick, 1999; Schmidberger and Francis, 1999; Kopylova and Russell, 2000).

The Renard dykes are highly enriched in terms of LREE compared to depleted mantle values (DMM; Workman and Hart, 2005), and display steep fractionated REE profiles (Ce/Yb ~ 400 ; Gd/Yb ~ 13 ; Fig. 8A). The Renard dykes are also highly enriched in HFSE (Th, U, Nb, Hf and Zr) and LILE elements (Rb, Ba, K and Sr) compared to DMM (Fig. 8B). Samples from the interior of the Lynx dyke have fractionated REE profiles and HFSE and LILE contents that are similar to those of the Renard dykes, but displaced to slightly lower total values (Fig. 8A and B). Although the aphanitic margins of the Lynx dyke have much higher incompatible element contents than the Lynx interiors, their trace element profiles are parallel. The trace element profiles of the interiors of Renard dykes and Lynx dyke are virtually identical to those of hypabyssal kimberlites from the Slave Province (Fig. 8A and B).

The Foxtrot kimberlites differ from other kimberlites in the region in having lower iron and titanium than those of the Lac Beaver and Tichegami kimberlites (Fe ~ 9 cat and Ti ~ 3 cat), and lower titanium than the Wemindji kimberlites (Ti ~ 3 cat; Hartzler, 2007). They also have higher Mg# (~ 88), with the highest Mg# (~ 91) associated with the highest olivine contents, found in the interior samples of the Lynx dyke. Furthermore, the highest diamond grades are found in Foxtrot kimberlites with the highest Mg# (Fig. 9). In comparison, kimberlites from Lac Beaver and Tichegami have a low Mg#'s (~ 83.5) and are non-diamondiferous (Moorhead et al., 2002; Letendre et al., 2003; Hartzler, 2007).

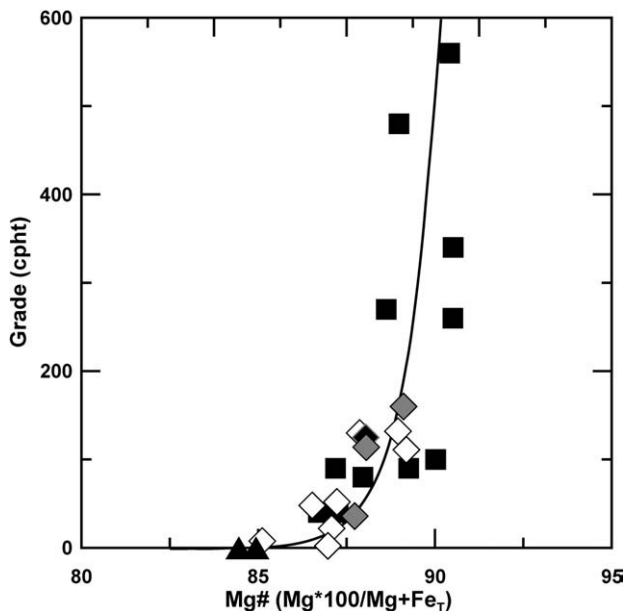


Fig. 9. Plot of diamond grade versus kimberlite whole rock Mg#. Renard kimberlite – white diamond; Lynx kimberlite – gray diamond; Hibou dyke – black diamond; Lac Beaver and Tichegami kimberlite – black triangle; Slave kimberlite – black square (Nowicki et al., 2008; Natural Resources Canada).

5. Discussion

The classification of kimberlite has a long and often complicated history with an ongoing debate as to whether Group II kimberlite (Smith, 1983; Smith et al., 1985) should even be called kimberlite, or re-classified

as orangite (Mitchell, 1995). African Group II kimberlites appear to represent a mixed population that includes olivine lamproites (Francis and Patterson, 2009). The official IUGS classification of igneous rocks states that kimberlite cannot be defined despite several attempts to classify them on the basis of mineralogy, radiogenic isotopes, or more recently facies models (Smith et al., 1985; Skinner, 1989; Mitchell, 1995; Le Maitre, 2002). The typical mineral assemblage for Group I kimberlite of Mitchell (1995) may include olivine, magnesian ilmenite, pyrope, diopside, phlogopite, enstatite and Ti-poor chromite as macrocrysts set in a fine-grained matrix having a mineralogy that may include olivine, monticellite, phlogopite, perovskite, spinel, apatite, carbonate and serpentine. In addition, Mitchell (1995) requires a Group I kimberlite to be volatile rich (dominantly CO₂), potassic, and ultrabasic. The Foxtrot kimberlites correspond to Mitchell's definition of kimberlite in that they are potassic, ultrabasic rocks that have common macrocrysts of olivine, ilmenite, rare pyrope, chrome-diopside and phlogopite set in a matrix of abundant carbonate complete with the matrix mineral assemblage.

The Renard kimberlites have previously been described as being intermediate between Group I kimberlite and melnoite or ultramafic lamprophyre (Birkett et al., 2004). This interpretation was based primarily on the composition of spinel and phlogopite that differ from the classical kimberlite trends outlined by Mitchell (1995) and Mitchell (1997). However, the Renard spinel compositions plot both along the magmatic Trend 1 in the reduced spinel prism, as well as between Trend 1 and Trend 2 (Supplementary Fig. 3). Furthermore, Mitchell (1995), and subsequent studies (Caro et al., 2004; Roeder and Schulze, 2008) have shown that Group I kimberlite can have spinels with a number of different compositional trends. Thus, spinel compositional trends do not appear to be diagnostic of Group I kimberlite, although Renard spinels are consistent with those observed in other kimberlites (i.e. Kirkland Lake).

Although the majority of phlogopite, in fresh Foxtrot samples fall in the field of kimberlite phlogopite as defined by Mitchell (1995), the compositions of the phlogopite in the rusty-orange margins of the Renard dykes trend towards iron-rich tetra-ferriphlogopite. The higher silicon contents and ubiquitous clinopyroxene microlites that characterize these samples are hallmark features of diatreme facies kimberlite (Skinner and Marsh, 2004). Previous studies of the transition from hypabyssal kimberlite to diatreme facies have demonstrated that the loss of CO₂ as a gas results in the crystallization of diopside and iron-rich phlogopite (Skinner and Marsh, 2004; Skinner, 2008). The fact that the rusty-orange

margin are juxtaposed with brecciated or diatreme facies kimberlite, rocks with a higher porosity than coherent kimberlite may indicate that late stage CO₂ degassing was responsible for the distinctive mineralogy of the rusty-orange margins.

Mantle $\delta^{13}\text{C}$ values (-5%) and magmatic textures indicate that carbonate in kimberlite is commonly a magmatic phase (Deines & Gold, 1973; Armstrong et al., 2004; Wilson et al., 2007; Francis and Patterson, 2009). The poikilitic texture of carbonate in the Foxtrot hypabyssal kimberlites indicates their primary magmatic nature and thus it is essential to include CO₂ when deciphering their whole rock compositional variations. When carbon is included in the cation calculation, it is clear that the Foxtrot hypabyssal kimberlite have silica contents that are less than that of olivine and have low-iron contents, as is typical of Group I kimberlites in general (Fig. 4; Francis and Patterson, 2009). Thus both the major and trace element composition of the Foxtrot hypabyssal dykes are typical of Group I kimberlite.

Although the importance of olivine is established by its abundance, its role in producing the chemical variation in the Foxtrot kimberlites is more enigmatic. The concomitant decrease in aluminium with decreasing magnesium and silicon effectively rules out olivine fractionation as being responsible for the geochemical variation of the macrocrystic interiors of the hypabyssal kimberlite of the Foxtrot Field. The overlap of the Mg#s and nickel content of Foxtrot olivine with those of olivine in mantle xenoliths carried by kimberlites indicates that the majority of olivine in the Foxtrot dykes is xenocrystic, sourced predominantly from mantle harzburgite (Fig. 2 and 3). Although this interpretation is consistent with the olivine to orthopyroxene ratio of $\sim 75/25$ indicated by whole rock variation of the PER analysis, the absence of orthopyroxene in the Foxtrot kimberlites requires that it is occult. Orthopyroxene is not stable in the presence of a hydrous carbonate-rich fluid (Eggler, 1973; Eggler et al., 1979) and has likely been assimilated by the kimberlite.

The increase in the size and abundance of olivine toward the interior of the Lynx dyke, along with their preferential alignment, are consistent with flow differentiation (Komar, 1972; Petford & Koenders, 1998). The cyclic banding and the parallel orientation of olivine in the aphanitic margins of the Lynx dyke suggest that these margins are successive coating of the conduit walls during fluid flow. The enrichment of major elements excluded from olivine (Al, Ti, K and P) and incompatible trace elements in the aphanitic margins of the Lynx dyke suggests that the majority of chemical variation between the margins and the interior of the dyke is due to olivine sorting during flow differentiation. The lack of

Table 1

Calculated composition of Renard kimberlite primary magma in comparison to other kimberlite magma estimates.

Renard magma (this work)				Literature estimates of kimberlite magma					
Oxide wt.%	Avg Renard	Renard ^a	Renard ^b	South Africa			Slave		
				Avg Group I	Kimberley	Uintjiesberg	Jericho		
				BLR ^c	Le Roex ^d	Harris ^e	JD69 ^f	JD82 ^f	296G-C (1) ^g
SiO ₂	35.03	27.24	24.33	29.38	30.57	27.31	29.77	31.32	29.61
TiO ₂	1.21	2.68	2.91	2.90	2.54	3.53	0.55	0.78	1.92
Al ₂ O ₃	2.44	5.49	5.92	3.10	2.54	2.53	1.43	1.78	1.74
MgO	34.86	16.87	15.15	28.34	30.56	28.50	24.69	25.72	31.34
FeO	8.32	8.58	8.90	10.85	10.15	10.01	5.94	7.38	8.41
MnO	0.15	0.21	0.22	0.21	–	0.21	0.15	0.18	0.20
CaO	9.43	20.31	22.23	14.90	13.84	16.38	21.40	18.60	14.31
Na ₂ O	0.06	0.10	0.10	0.18	–	0.07	0.17	0.21	0.11
K ₂ O	0.79	1.82	1.96	0.93	1.73	2.04	0.44	0.56	1.40
P ₂ O ₅	0.42	0.93	1.03	–	–	–	–	–	–
CO ₂	7.28	15.77	17.25	9.21	8.07	9.43	15.46	13.47	10.96
Total	100	100	100	100	100	100	100	100	100
Mg#	0.88	0.78	0.75	0.82	0.84	0.84	0.88	0.86	0.87

^a Composition calculated by removal of olivine mineral composition from whole rock data.

^b Composition calculated by removal of equivalent proportion of orthopyroxene.

^c Becker and Roex (2006).

^d Le Roex et al. (2003).

^e Harris et al. (2004).

^f Price et al. (2000).

^g Kopylova et al. (2007) (composition before orthopyroxene assimilation).

volcanoclastic kimberlite and common oikocrystic calcite exhibited within the Lynx dyke suggests a slower cooling rate than kimberlites that would lose heat during surface eruption. The complete serpentinization of olivine in the Lynx dyke suggests the prolonged presence of late stage water-rich fluid is likely responsible for some of the chemical variation between the interiors and margins of the dyke (i.e. iron remobilization). The almost constant carbon contents from the interiors to the margins of the Lynx dyke are also inconsistent with flow differentiation, since this process should result in an increase in carbonate in the margins. The presence of carbonate veining and serpentinization in the country rock juxtaposed to the Lynx dyke suggests the possibility that carbonate may have been lost to the surrounding country rock.

The xenocrystic nature of olivine in the Foxtrot kimberlites indicates that the entrained olivine should be removed to estimate the actual magma composition. The absence of any correlation between olivine composition and crystal size indicates that the fine-grained olivine in the matrix is also xenocrystic and should be removed, but this is not possible to do mechanically during sample preparation. The restricted mineral chemistry of the olivine in the Foxtrot kimberlite does, however, allow the mathematical removal of the modal amount (30 to 70%, average 55%) of olivine from each of the whole rock composition. The calculation results in a composition has much lower silica (~27 wt.%) and magnesium contents (~17 wt.%) than the whole rock compositions (~35 and 35 wt.% respectively; Table 1). The contribution of the assimilated harzburgitic orthopyroxene is more enigmatic due to the absence of orthopyroxene in the Foxtrot kimberlites, but an olivine/orthopyroxene ratio similar to that of the harzburgite mantle xenoliths (80/20) can be used to remove an equivalent proportion of orthopyroxene which reduces the estimated silica content of the magma to ~24 wt.% and raises its estimated CO₂ content to 17 wt.% cat (Table 1). Although this composition is lower in silica and significantly richer in CO₂ compared to previous magma estimates, the calculated magma composition has only half the MgO contents (~15 wt.%) compared to previous estimates (~24 to 31 wt.%). This simply reflects that the majority of olivine and subsequent orthopyroxene is xenocrystic in the Foxtrot kimberlites, whereas approximately half of the olivine is considered xenocrystic in the previous studies.

The majority of the major element variation in the Foxtrot kimberlites can thus be produced by mixing of 40 to 70% refractory mantle with a carbonate-rich liquid. The correlation between diamond grade whole rock Mg#’s and lowest titanium contents in the Foxtrot Kimberlite Field extends to the other kimberlites in the Otish Mountains, such as the non-diamondiferous Lac Beaver and Tichegami kimberlites (Fig. 9) which are characterized by low Mg# and high Ti contents. Furthermore, a survey of Slave province kimberlites indicates a similar correlation between Mg#, Ti content and diamond grade, suggesting that this correlation is a global feature of kimberlites. A harzburgite and carbonate-rich magma mixture model for the Foxtrot kimberlites suggests that the correlation between whole rock composition and diamond grade may simply reflect the fact that the diamonds are also xenocrystic and are most abundant in kimberlite that has the highest proportion of refractory harzburgite (Francis and Patterson, 2009). Whole rock chemistry (i.e. Mg# and Ti content) provides an inexpensive tool with which to estimate diamond grade that could enhance diamond exploration strategies.

6. Conclusions

Carbonate is a magmatic phase in the Foxtrot kimberlites and must be included in a petrogenetic interpretation of their chemical compositions. The whole rock compositions of the Foxtrot hypabyssal kimberlites are best explained by a model in which a hydrous carbonate-rich fluid interacts with and entrains refractory cratonic harzburgite. The entrained cratonic mantle material remains as rounded olivine xenocrysts, whereas the mantle orthopyroxene has been assimilated by the carbonate-rich fluid. The removal of harzburgite component from the whole rock

compositions yields an estimated magma composition that is poor in SiO₂ and MgO (~24 and 15 wt.% respectively), but rich in CO₂ rich (~17 wt.%) compared to the estimates of previous studies (Price et al., 2000; Le Roex et al., 2003; Harris et al., 2004; Kopylova et al., 2007; Becker and Roex, 2006;). The correlation of the highest diamond grades and the highest Mg# and lowest Ti content, in the Foxtrot kimberlite is interpreted to reflect the greater abundance of refractory harzburgite that has been entrained, coupled with the preferential development of diamonds in highly refractory mantle lithosphere.

Acknowledgements

Whole rock XRF analyses for major elements and select trace elements (Ni, V, Ga, Nb, Rb, Sr, Th, U, Y, and Zr) were performed at the Geochemical Laboratories at McGill University. Electron Microprobe analysis was completed under the guidance of Shi Lang at McGill University. This manuscript benefited greatly from reviews by Dr. Robert Luth, Dr. Kelly Russell and Dr. Dan Schulze. This research was funded by a Collaborative Research and Development grant (CRDPJ 342496-06) from the Natural Science and Engineering Research Council of Canada in collaboration with Stornoway Diamond Corporation.

Appendix A. Supplementary data

Supplementary data associated with this article can be found, in the online version, at doi:10.1016/j.lithos.2009.06.004.

References

- Armstrong, J.P., Wilson, M., Barnett, R.L., Nowicki, T., Kjarsgaard, B.A., 2004. Mineralogy of primary carbonate-bearing hypabyssal kimberlite, Lac de Gras, Slave Province, Northwest Territories, Canada. *Lithos* 76, 415–433.
- Becker, M., Roex, A.P.L., 2006. Geochemistry of South African on- and off-craton, Group I and Group II kimberlites: petrogenesis and source region evolution. *Journal of Petrology* 47, 673–703.
- Birkett, T.C., McCandless, T.E., Hood, C.T., 2004. Petrology of the Renard igneous bodies: host rocks for diamond in the northern Otish Mountains region, Quebec. *Lithos* 76, 475–490.
- Boyd, F.R., 1987. High- and low-temperature garnet peridotite xenoliths and their possible relation to the lithosphere – asthenosphere boundary beneath southern Africa. In: Nixon, P.H. (Ed.), *Mantle Xenoliths*. Wiley, Chichester, pp. 403–412.
- Boyd, F.R., Pokhilenko, N.P., Pearson, D.G., Mertzman, S.A., Sobolev, N.V., Finger, L.W., 1997. Composition of the Siberian cratonic mantle: evidence from Udachnaya peridotite xenoliths. *Contributions to Mineral Petrology* 128, 228–246.
- Caro, G., Kopylova, M.G., Creaser, R.A., 2004. The hypabyssal 5034 kimberlite gahcho kue cluster, Southeastern Slave Craton, Northwest Territories, Canada: a granite-contaminated group-I kimberlite. *The Canadian Mineralogist* 42, 183–207.
- Carswell, D.A., Clarke, D.B., Mitchell, R.H., 1979. The petrology and geochemistry of ultramafic nodules from Pipe 200, northern Lesotho. In: Boyd, F.R., Meyers, H.O.A. (Eds.), *Proc. Sec. Inter. Kimberlite Conf. 2*. AGU, Washington, DC, pp. 127–144.
- Clement, C.R., 1982. A comparative geological study of some major kimberlite pipes in the northern Cape and Orange Free State. Unpublished PhD thesis, University of Cape Town, South Africa, 431.
- Clements, B., O’Connor, A., 2002. Quebec technical report May 17, 2002. Ashton Mining of Canada Annual Technical Report.
- Deines, P., Gold, D.P., 1973. The isotopic composition of carbonatite and kimberlite carbonates and their bearing on the isotopic composition of deep-seated carbon. *Geochimica et Cosmochimica Acta* 37, 1709–1733.
- Eggler, D.H., 1973. Role of CO₂ in melting processes in the mantle. *Carnegie Institute of Washington Yearbook*, 1972–73, 457–467.
- Eggler, D.H., Kushiro, I., Holloway, J.R., 1979. Free energies of decarbonation reactions at mantle pressures: I. Stability of the assemblage forsterite–enstatite–magnesite in the system MgO–SiO₂–CO₂–H₂O to 60 kbar. *American Mineralogist* 64, 288–293.
- Fedorchouk, Y., Canil, D., 2004. Intensive variables in kimberlite magmas, Lac de Gras, Canada and implications for diamond survival. *Journal of Petrology* 45, 1725–1745.
- Fitzgerald, C.E., et al., 2009, this issue. The internal geology and emplacement history of the Renard 2 kimberlite, Superior Province, Quebec, Canada. Proceedings of the 9th International Kimberlite Conference. *Lithos* 112S, 513–528.
- Francis, D., 2003. Implications of major element composition for the mantle sources of kimberlite, aillikite, olivine lamproite and meimechite. Extended Abstracts of the 8th International Kimberlite Conference, Victoria, Canada, 2003.
- Francis, D., Patterson, M., 2009. Kimberlites and Aillikites as Probes of the Continental Lithospheric Mantle. *Lithos* 109, 72–80.
- Girard, R., 2001. Caractérisation de l’intrusion Kimberlitique du lac Beaver, Monts Otish–Petrographie et Mineralogy. Ressources Naturelles Quebec, Government Province Quebec, Canada, MB. 2001-08, 23 pp.

- Goffon, 2007. The Renard 4 Kimberlite: Implications for ascent of kimberlites in the shallow crust. Unpublished Msc Thesis, University of British Columbia, Vancouver, British Columbia, Canada.
- Harris, M., Le Roex, A., Class, C., 2004. Geochemistry of the Uintjiesberg kimberlite, South Africa: petrogenesis of an offcraton, Group I kimberlite. *Lithos* 74 (3–4), 149–165.
- Hartzler, J.R., 2007. The geological exploration of kimberlitic rocks in Quebec. Unpublished Msc Thesis, McGill University, Montreal, Quebec, Canada.
- Hawthorne, J.B., 1975. Model of a kimberlite pipe. *Physics and chemistry of the earth*. In: Ahrens, L., et al. (Ed.), *Proceedings of the 1st International Kimberlite Conference: Physics and Chemistry of the Earth*, vol. 9, pp. 1–15.
- Komar, P.D., 1972. Flow differentiation in igneous dikes and sills: profiles of velocity and phenocryst concentration. *Geological Society of America Bulletin*, vol. 83, No. 11, pp. 3443–3448.
- Kopylova, M.G., Russell, J.K., 2000. Chemical stratification of cratonic lithosphere: constraints from the northern Slaver craton, Canada. *Earth and Planetary Science Letters* 181, 71–87.
- Kopylova, M.G., Matveev, S., Raudsepp, M., 2007. Searching for parental kimberlite melt. *Geochimica et Cosmochimica Acta* 71, 3616–3629.
- Le Maitre, R.W., 2002. Igneous rocks, a classification and glossary of terms: recommendations of the International Union of Geological Sciences. Subcommission on the Systematics of Igneous Rocks, In: Le Maitre, R.W. (Ed.), 2nd Edition. Cambridge University Press.
- Le Roex, A.P., Bell, D.R., Davis, P., 2003. Petrogenesis of Group I kimberlites from Kimberley, South Africa: evidence from bulk-rock geochemistry. *Journal of Petrology* 44, 2261–2286.
- Lee, C.T., Rudnick, R.L., 1999. Compositionally stratified cratonic lithosphere: petrology and geochemistry of peridotite xenoliths from the Labait volcano, Tanzania. *Proc. 7th Inter. Kimberlite. Red Roof Design*, Cape Town, South Africa, pp. 503–521.
- Letendre, J., L'Heureux, M., Nowicki, T.E., Creaser, R., 2003. The Wemindji kimberlites: exploration and geology. (Extended Abstract) Programme and Abstracts of the 8th International Kimberlite Conference.
- McCandless, T., Schulze, D., Bellis, A., Taylor, L.A., Liu, Y., van Rythoven, A.D., 2008. Morphology and chemistry of diamonds from the lynx kimberlite dyke complex, Northern Otish Mountains, Quebec. Extended Abstracts of the 9th International Kimberlite Conference, Frankfurt, Germany. August, 2008.
- Mitchell, R.H., 1995. Kimberlites, orangeite, and related rocks. Plenum Press, New York.
- Mitchell, R.H., 1997. Kimberlites, Orangeites, Lamproites, Melilitites, and Minettes: a Petrographic Atlas. Almaz Press Inc, Thunder Bay, Ontario, Canada.
- Moorhead, J., Giriard, R., Heaman, L., 2002. Characterisation des Kimberlites au Quebec. Ministère des Ressources naturelles du Quebec. Government Province Quebec, Canada, DV, pp. 2002–2010. 36 pp.
- Nixon, P.H., Boyd, F.R., 1973. Petrogenesis of the granular and sheared ultrabasic nodule suite in kimberlites. *Lesotho Kimberlites*, pp. 48–56.
- Nowicki, T., Porritt, L., Crawford, B., Kjarsgaard, B., 2008. Geochemical trends in kimberlites of the Ekati property, Northwest Territories, Canada: insights on volcanic and resedimentation processes. *Journal of Volcanology and Geothermal Research* 174, 117–127.
- Pearce, T.H., 1968. A contribution to the theory of variation diagrams. *Contributions to Mineralogy and Petrology* 19, 142–157.
- Petford, N., Koenders, M.A., 1998. Granular flow and viscous fluctuations in low Bagnold number granitic magmas. *Journal of the Geological Society, London* 155, 873–881.
- Price, S.E., Russell, J.K., Kopylova, M.G., 2000. Primitive magma from the Jericho Pipe, N.W.T., Canada: constraints on primary kimberlite melt chemistry. *Journal of Petrology* 41, 789–808.
- Roeder, P.L., Schulze, D.J., 2008. Crystallization of groundmass spinel in kimberlite. *Journal of Petrology* 49 (8), 1473–1495.
- Russell, J.K., Nicholls, J., 1988. Analysis of petrologic hypotheses with Pearce element ratios. *Contributions to Mineralogy and Petrology* 99, 25–35.
- Schmidberger, S.S., Francis, D., 1999. Nature of the mantle roots beneath the North American Craton: mantle xenolith evidence from Somerset Island kimberlites. *Lithos* 48, 195–216.
- Schmidberger, S.S., Francis, D., 2001. Constraints on the trace element composition of the Archean mantle root beneath Somerset Island, Arctic Canada. *Journal of Petrology* 42, 1095–1117.
- Sheppard, S.M.F., Dawson, J.B., 1975. Hydrogen, carbon, and oxygen isotope studies of megacryst and matrix minerals from Lesotho and South African kimberlites. *Physics and Chemistry of the Earth* 9, 747–763.
- Skinner, E.M.W., 1989. Contrasting Group 1 and Group 2 kimberlite petrology: towards a genetic model of kimberlites. In: Ross, J., Jaques, A.L., Ferguson, J., Green, D.H., O'Reilly, S.Y., Danchin, R.V., Janse, A.J.A. (Eds.), *Kimberlites and Related Rocks: Geological Society of Australia*, vol. 14, pp. 528–544. Sydney.
- Skinner, E.M.W., 2008. The emplacement of class 1 kimberlites. *Journal of Volcanology and Geothermal Research* 174 (Issues 1–3), 40–48 Kimberlite Emplacement.
- Skinner, E.M.W., Marsh, J.S., 2004. Distinct kimberlite pipe classes with contrasting eruption processes. *Lithos* 76, 183–200.
- Smith, C.B., 1983. Pb, Sr and Nd isotopic evidence for sources of southern African Cretaceous kimberlites. *Nature* 304, 51–54.
- Smith, C.B., Gurney, J.J., Skinner, E.M.W., Clement, C.R., Ebrahim, N., 1985. Geochemical character of southern African kimberlites: a new approach based on isotopic constraints. *Transactions of the Geological Society South Africa* 88, 180–267.
- Stripp, G.R., Field, M., Schumacher, J.C., Sparks, R.S.J., Cressey, G., 2006. Post-emplacement serpentinization and related hydrothermal metamorphism in a kimberlite from Venetia, South Africa. *Journal of Metamorphic Petrology* 24, 515–534.
- Vasilenko, V.B., Zinchuk, N.N., Krasavchikov, V.O., Kuznetsova, L.G., Khlestov, V.V., Volkova, N.I., 2002. Diamond potential estimation based on kimberlite major element chemistry. *Journal of Geochemical Exploration* 79, 93–112.
- Wilson, M.R., Kjarsgaard, B.A., Taylor, B., 2007. Stable isotope composition of magmatic and deuteric carbonate phases in hypabyssal kimberlite, Lac de Gras field, Northwest Territories, Canada. *Chemical Geology* 242, 435–454.
- Woolley, A.R., Kempe, D.R.C., 1989. Carbonatites: nomenclature, average chemical compositions and element distribution. In: Bell, K. (Ed.), *Carbonatites – Genesis and Evolution*. Unwin Hyman, pp. 1–14.
- Workman, R.K., Hart, S.R., 2005. Major and trace element composition of the depleted MORB mantle (DMM). *Earth and Planetary Science Letters* 231, 53–72.